

Detecting competing orders through the edge states in the heterostructures with high- T_c superconductors

Tao Zhou,^{1,2,*} Yi Gao,³ and Z. D. Wang^{4,†}¹*Guangdong Provincial Key Laboratory of Quantum Engineering and Quantum Materials, and School of Physics and Telecommunication Engineering, South China Normal University, Guangzhou 510006, China*²*College of Science, Nanjing University of Aeronautics and Astronautics, Nanjing 210016, China*³*Department of Physics and Institute of Theoretical Physics, Nanjing Normal University, Nanjing 210023, China*⁴*Department of Physics and Center of Theoretical and Computational Physics, The University of Hong Kong, Pokfulam Road, Hong Kong, China*

(Received 14 October 2018; published 26 March 2019)

We here propose a feasible method to detect hidden orders in high- T_c superconductors. When we consider a d -wave superconductor being in proximity to a two-dimensional Weyl model, a topological superconductor with gapless edge states may be realized. The system can become topologically trivial when an additional d -density-wave order is also included. The edge states become gapped and may be detected in experiments. For this, the d -density-wave order can be detected experimentally, and different scenarios for the pseudogap in high- T_c superconductors may be distinguished. This method may be used to detect various hidden orders through putting high- T_c superconductors being in proximity to designated topologically nontrivial materials.

DOI: [10.1103/PhysRevB.99.104517](https://doi.org/10.1103/PhysRevB.99.104517)

I. INTRODUCTION

Although the high- T_c superconductivity was discovered in cuprate materials more than 30 years ago [1], no consensus has so far been reached regarding its mechanism. This is partially due to lack of a profound understanding of pseudogap states [2–8]. Generally, there are two different scenarios for the pseudogap states, according to the relationship between the pseudogap and the superconducting pairing gap. One is the phase fluctuation scenario, suggesting that the pseudogap is due to the preformed Cooper pairs [4]. The other lies in that the pseudogap may be due to certain competing hidden orders [5–8]. Actually, the existence of possible competing orders in high- T_c superconductors is a rather important issue. Now it was widely believed that multiple competing orders may exist, and they are not limited to explaining the pseudogap phenomenon [6–10]. Identifying various orders in the superconducting state is important and we may find a useful clue in searching for the real origin of superconductivity.

Recently, research on topological superconductors has also attracted tremendous interest [11]. A topological superconductor is characterized by a full superconducting gap in the bulk and topologically protected gapless states at the system edges. The edge states are in connection with the Majorana bound states, which obey non-Abelian statistics and have potential applications in topological quantum computation [12]. Notably, most previous efforts have been made in searching for topological superconductors and Majorana bound states. It was proposed theoretically that an effective topological superconductor may be realized in the heterostructure system, e.g.,

the superconductor is in proximity to a topological insulator [13], quantum anomalous insulator [14], or a semiconductor with the spin-orbital coupling [15–17]. Experimentally, the above heterostructure systems were indeed realized and possible signatures of Majorana bound states were reported in these systems [18–25]. On the other hand, since the high- T_c superconductors have a much larger pairing gap, it is natural to consider whether the topological superconductor can be realized in the high- T_c superconductor families. So far, the cuprate-based heterostructure has been studied intensively [26–30], and several signatures of proximity induced superconductivity were indeed probed experimentally [26,27]. It was also indicated theoretically and verified experimentally that the iron-based superconductors may provide another platform based on high- T_c superconductors for realizing topological superconductors [31–35].

In this paper we elucidate that the topological heterostructure may provide a useful platform to detect and resolve the possible competing orders in high- T_c superconductors. As is known, in the superconducting state of high- T_c superconductors, it may be rather difficult to detect the possible competing orders because such order is normally covered up by the superconducting gap. Even in the case that some signatures of certain order are seen, it is still difficult to determine its physical origin because the energy spectrum may be qualitatively the same for different theoretical scenarios. While in the topological system, there exist gapless edge states, such that even if the bulk states are similar to each other for different orders, the edge states can be significantly different. Thus we may be able to resolve different competing orders through studying the edge states. Especially, the topological protected features may be sensitive to a certain competing order, which may be exploited to determine the physical origin of the pseudogap behavior and to probe some weak hidden orders.

*tzhou@scnu.edu.cn

†zwang@hku.hk

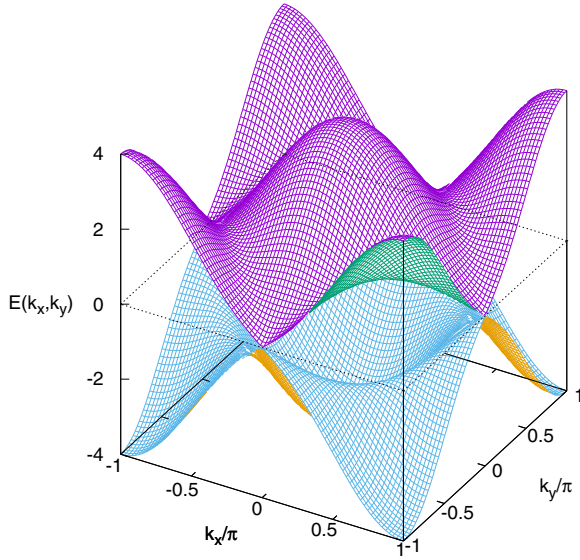


FIG. 1. The normal state energy bands from the Hamiltonian of Eq. (1).

The rest of the paper is organized as follows. In Sec. II we introduce the model and present the relevant formalism. In Sec. III we report numerical calculations and discuss the obtained results. Finally, we give a brief summary in Sec. IV.

II. MODEL AND FORMALISM

To demonstrate our proposal, we start from a two-dimensional lattice Weyl model, given by

$$H_N = \sum_{\mathbf{k}\sigma} \varepsilon_{\mathbf{k}\sigma} c_{\mathbf{k}\sigma}^\dagger c_{\mathbf{k}\sigma} + \sum_{\mathbf{k}} (\lambda_{\mathbf{k}} c_{\mathbf{k}\uparrow}^\dagger c_{\mathbf{k}\downarrow} + \text{H.c.}), \quad (1)$$

with $\varepsilon_{\mathbf{k}\sigma} = -2\sigma t(\cos k_x + \cos k_y)$ being a spin polarized hopping term. $\lambda_{\mathbf{k}} = 2\lambda_0(\sin k_x + i \sin k_y)$ corresponds to a spin-orbital coupling. Then we can obtain two energy bands with $E(k_x, k_y) = \sqrt{\varepsilon_{\mathbf{k}\sigma}^2 + |\lambda_{\mathbf{k}}|^2}$. These two bands as functions of the momentums are plotted in Fig. 1. The Weyl points at the positions $(\pm\pi, 0)$ and $(0, \pm\pi)$ are seen clearly. The above Hamiltonian may be realized in the HgTe/CdTe quantum well system [36,37], or the single layer LaCl/LaBr materials [38].

In proximity to a cuprate high- T_c superconductor, the d -wave superconducting (DSC) pairing term is induced to the system. We also consider a competing d -density-wave (DDW) order, which was proposed to describe the pseudogap state in the underdoped high- T_c cuprates [5].

The Hamiltonian of the DSC and DDW parts are expressed as

$$H_{\text{DSC}} = \sum_{\mathbf{k}} \Delta_{\mathbf{k}} (c_{\mathbf{k}\uparrow}^\dagger c_{-\mathbf{k}\downarrow}^\dagger + \text{H.c.}) \quad (2)$$

and

$$H_{\text{DDW}} = \sum_{\mathbf{k}\sigma} W_{\mathbf{k}} (c_{\mathbf{k}\sigma}^\dagger c_{\mathbf{k}+\mathbf{Q}\sigma}), \quad (3)$$

where $\mathbf{Q} = (\pi, \pi)$, $\Delta_{\mathbf{k}} = 2\Delta_{\text{DSC}}(\cos k_x - \cos k_y)$, and $W_{\mathbf{k}} = 2i\Delta_{\text{DDW}}(\cos k_x - \cos k_y)$.

We define the topological invariant \mathcal{N} expressed as

$$\mathcal{N} = \frac{1}{2\pi} \iint \left[\frac{\partial a_y(\mathbf{k})}{\partial k_x} - \frac{\partial a_x(\mathbf{k})}{\partial k_y} \right] dk_x dk_y, \quad (4)$$

with

$$a_\alpha(\mathbf{k}) = -i \sum_{m \in \text{occ}} \langle u_m(\mathbf{k}) | \frac{\partial}{\partial k_\alpha} | u_m(\mathbf{k}) \rangle, \quad (5)$$

where $|u_m(\mathbf{k})\rangle$ is the eigenstate of the occupied state m .

To study the edge states, we define a partial Fourier transformation along the x direction with $C_{\mathbf{k}}^\dagger = \frac{1}{\sqrt{N_x a}} \sum_x C_{k_y}^\dagger(x) e^{ik_x x}$. The Hamiltonian is reduced to the quasi-one-dimensional one, which can be rewritten as

$$\begin{aligned} H_N = & -t \sum_{k_y, x, \sigma} [\sigma c_{k_y, \sigma}^\dagger(x) c_{k_y, \sigma}(x+a) + \text{H.c.}] \\ & - i\lambda_0 \sum_{k_y, x} [c_{k_y, \uparrow}^\dagger(x) c_{k_y, \downarrow}(x+a) + \text{H.c.}] \\ & - 2t \sum_{k_y, x, \sigma} \sigma \cos k_y c_{k_y, \sigma}^\dagger(x) c_{k_y, \sigma}(x) \\ & + 2i\lambda_0 \sum_{k_y, x} \sin k_y c_{k_y, \uparrow}^\dagger(x) c_{k_y, \downarrow}(x), \end{aligned} \quad (6)$$

with a being the lattice constant along the x direction.

The Hamiltonian for the DSC pairing and DDW parts are rewritten as

$$\begin{aligned} H_{\text{DSC}} = & \sum_{k_y, x} [\Delta_{\text{DSC}} c_{k_y, \uparrow}^\dagger(x) c_{-k_y, \downarrow}^\dagger(x \pm a) + \text{H.c.}] \\ & - \sum_{k_y, x} [2\Delta_{\text{DSC}} \cos k_y c_{k_y, \uparrow}^\dagger(x) c_{-k_y, \downarrow}^\dagger(x) + \text{H.c.}] \end{aligned} \quad (7)$$

and

$$\begin{aligned} H_{\text{DDW}} = & - \sum_{k_y, x, \sigma} [i\Delta_{\text{DDW}} c_{k_y, \sigma}^\dagger(x) c_{k_y + \pi, \sigma}(x+a) + \text{H.c.}] \\ & - \sum_{k_y, x, \sigma} [2i\Delta_{\text{DDW}} \cos k_y c_{k_y, \sigma}^\dagger(x) c_{k_y + \pi, \sigma}(x)]. \end{aligned} \quad (8)$$

The whole Hamiltonian can be written as $4N_x \times 4N_x$ or $8N_x \times 8N_x$ (with the DDW order) matrix form. Then the x -dependent spectral functions $A_x(k_y, \omega)$ and the local density of states $\rho_x(\omega)$ can be calculated from the imaginary part of the Green's function, expressed as

$$A_x(k_y, \omega) = \sum_{n, \sigma} \frac{|u_{x\sigma}^n(k_y)|^2}{\omega - E_n(k_y) + i\Gamma} \quad (9)$$

and

$$\rho_x(\omega) = \frac{1}{N_y} \sum_{k_y} A_x(k_y, \omega). \quad (10)$$

Γ is a small infinitesimal quantity which is usually induced to make the Green's function converge. $u_{x\sigma}^n$ and $E_n(\mathbf{k})$ are eigenvectors and eigenvalues through diagonalizing the Hamiltonian matrix.

In the following, we take the nearest-neighbor hopping t and the lattice constant a as the energy and length units. The

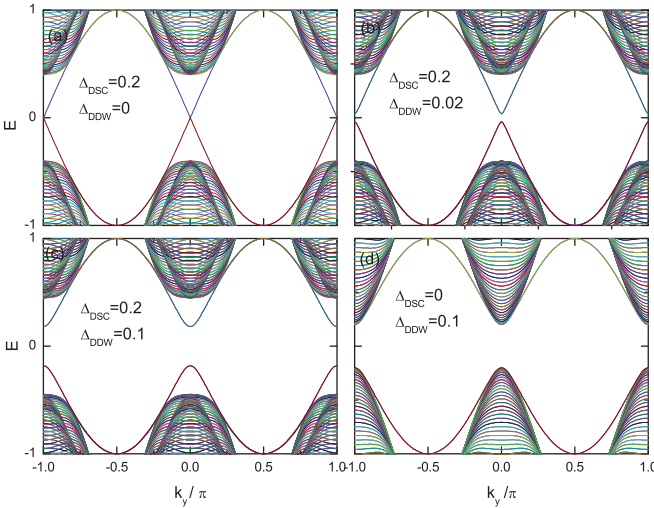


FIG. 2. Energy eigenvalues of the Hamiltonian in different states [a pure DSC state (a), the coexistence states (b) and (c), and a pure DDW state (d)], with the open boundary condition along x direction being considered.

other input parameters are chosen as $\lambda_0 = 0.5$ and $\Gamma = 0.01$. We have checked numerically that our main results are not sensitive to the parameters.

III. RESULTS AND DISCUSSION

We first study the energy spectra of different states, including the pure DSC state, the DDW state, and the state in which the DSC order and the DDW order coexist. Note that the bulk energy bands from all three states are fully gapped and a topological invariant [Eq. (4)] is well defined. We now study numerically the edge states of these three states through considering the open boundary condition along the x direction with $1 \leq x \leq 100$. Here the system size is large enough for observing the edge states and our main results are qualitatively the same when the open boundary rotates to other directions. The numerical results of the energy bands for the reduced quasi-one-dimensional Hamiltonian are presented in Fig. 2. In the pure DSC state with $\Delta_{\text{DDW}} = 0$, as is seen in Fig. 2(a), there are in-gap edge states crossing the Fermi energy at the momentum $k_y = 0$ and $k_y = \pi$. The edge states connect the upper and lower energy bands, indicating that the system may be a topological superconductor. The energy bands for the coexisting state are displayed in Figs. 2(b) and 2(c). For this case, the energy bands at the system edges are also fully gapped, with the gap magnitude depending on the DDW intensity. For the energy band of the pure DDW state, as presented in Fig. 2(d), it is also fully gapped for both system bulk and system edge. Thus for both the coexisting state and the pure DDW state, the system is topologically trivial. This result may be used to detect the DDW order experimentally. The numerical results for the energy spectra are consistent with the numerical calculations of the topological invariant. For the pure DSC state, the topological invariant \mathcal{N} equals 2 obtained from Eq. (4), corresponding to the two unequal Weyl points at the momentums $(0, \pi)$ and $(\pi, 0)$ shown in Fig. 1. When the DDW term is added, the topological invariant

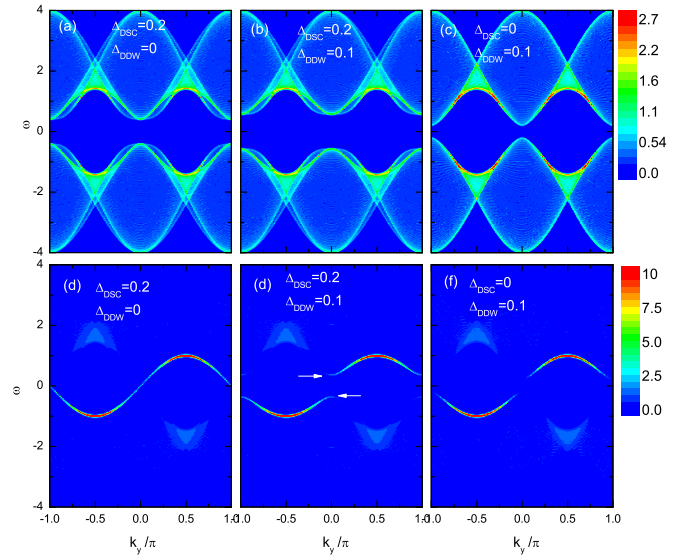


FIG. 3. The intensity plots of spectral functions at the system bulk (a)–(c) and the system edge (d)–(f) for different states.

immediately turns to zero, as a result, the energy bands at the system edge are also fully gapped.

Experimentally, the possible edge states may be detected by the angle-resolved photoemission spectroscopy (ARPES) experiments [39] or the scanning tunneling microscopy (STM) techniques [40]. The results of these two experiments can be described theoretically by the spectral function [Eq. (9)] and the LDOS [Eq. (10)], respectively. We first study numerically the spectral function with the open boundary condition along the x direction with $1 \leq x \leq 100$. The intensity plots of the spectral functions for the three different states in the system bulk and at the system edge are presented in Fig. 3. In the system bulk with $x = 50$ [Figs. 3(a)–3(c)], the spectra are fully gapped for all three states considered. It seems that there is no significant difference between the bulk spectra of different states. Especially when the DDW order coexists with the DSC order, the spectrum is almost the same as that of the pure DSC state, as seen in Figs. 3(a) and 3(b). Here the DDW gap is indeed covered up, and thus it seems rather difficult to detect such a gap merely from the bulk spectra.

We now turn to address the edge states of these three states. The numerical results for the spectral functions at the system edge ($x = 1$) are presented in Figs. 3(d)–3(f). In the pure DSC state [Fig. 3(d)], there are gapless edge states crossing the Fermi energy. While when a DDW term is added [Fig. 3(e)], the edge states end up at a nonzero finite energy, indicated by the arrows. An obvious energy gap is seen clearly. In the pure DDW state [Fig. 3(f)], an obvious energy gap is also seen clearly. Therefore, the existence of the DDW order may indeed be detected from the edge states by ARPES experiments.

Now we study the LDOS spectra. Considering the open boundary along the x direction, the LDOS from the system bulk to the system edge are plotted in Fig. 4. First let us look at the spectra in the system bulk. The intensities reach zero value at low energies for all three states, indicating the fully gapped feature. Also, in the coexisting state, the DDW gap

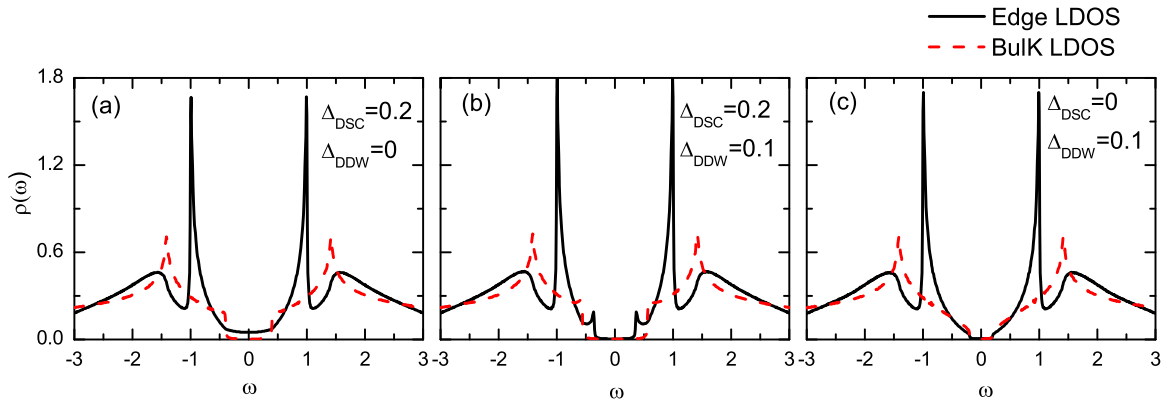


FIG. 4. The LDOS for different states for a two-dimensional system.

is almost hidden by the DSC gap and may be difficult to be detected experimentally.

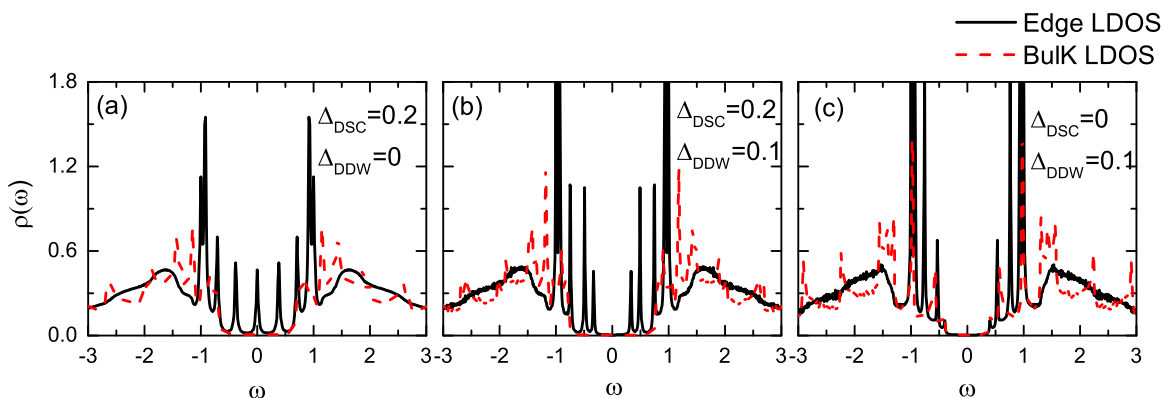
Let us study the LDOS spectra at the system edge. In the pure DSC state, as is seen in Fig. 4(a), the LDOS intensities at low energies are nonzero, due to the gapless edge states. While when an additional DDW order is added to the system [Fig. 4(b)], the low energy intensities recover to the zero value. Especially, there exist two obvious low energy peaks lying symmetric at the two sides of the Fermi energy. These two low energy peaks are corresponding to the energy gap opened by the DDW term at the system edge, as indicated by arrows in Fig. 3(e). This additional gap feature can be seen clearly from the LDOS spectrum in the coexisting state. In the pure DDW state [Fig. 4(c)], the LDOS spectrum is fully gapped and no in-gap features exist.

We wish to indicate that it may be difficult to use the above LDOS spectra for resolving different states in real materials. The whole system is a multiband system and some low energy peaks may be proximity induced. Moreover, here the LDOS spectrum at the system edge has no zero energy peak even for a topologically nontrivial superconducting state, as presented in Fig. 4(a). Actually, this result is understandable because the low energy edge states in a two-dimensional system are continuous crossing the Fermi energy. The small nonzero values at low energies are difficult to be resolved in real materials. It may also be due to finite temperature

smoothing or some other possible broadening effect. On the other hand, note that in a quasi-one-dimensional topological superconductor, usually the low energy edge states are the zero energy bound states protected by a minigap [41]. As a result, the LDOS at the system edge should have a sharp peak at zero energy. We here propose that we can consider the system with a DSC cuprate superconductor being coupled to a quasi-one-dimensional semimetal system. Then the LDOS spectra for the pure DSC state should be significantly different from the other two states and may be resolved by the STM experiments.

We plot, in Fig. 5, the LDOS spectra of different states for the system size 200×8 with the open boundary condition along the x direction. In the system bulk with $x = 100$, the LDOS spectra are fully gapped at low energies for all three states we considered. While at the system edge with $x = 1$, as is seen in Fig. 5(a), there is one zero energy peak and two symmetric low energy peaks in the pure DSC state. When the DDW order is added to the system, as is seen in Figs. 5(b) and 5(c), the zero energy peak disappears. Thus for the quasi-one-dimensional system, the pure DSC state may be distinguished from the state with the DDW order. In this way, the existence of the DDW order may be detected by the STM experiments.

We have demonstrated that the topological property varies when a DDW order is added, so that the existence of the DDW order may be detected through investigating the edge states.

FIG. 5. The LDOS for different states for a quasi-one-dimensional lattice with the system size 200×8 .

The size effect is also checked numerically and our results do not change as the system size increases. The spectra at the system edge recovers to the bulk value when four lattices away from the system edge. We also studied the disordered effect and confirmed that the disorder does not affect the main results.

Our main results about the topological features can be understood through block diagonalizing the Hamiltonian. In the pure superconducting state, as have been verified in Ref. [42], one may define two spinless operators, then the system is equivalent to a two-band $p + ip$ superconductor with the same chirality, with the spin-orbital coupling term $\lambda_{\mathbf{k}}$ turns to the quasiparticle pairing term. As a result, the system should be a topological superconductor.

In the presence of the DDW order, we start from the 4×4 nonsuperconducting Hamiltonian in the momentum space with $\Delta_{\text{DSC}} = 0$. Defining the quasiparticles $\alpha_{\mathbf{k}\sigma}$ and $\beta_{\mathbf{k}\sigma}$, with

$$\begin{pmatrix} \alpha_{\mathbf{k}\sigma} \\ \beta_{\mathbf{k}\sigma} \end{pmatrix} = \begin{pmatrix} u_{\mathbf{k}\sigma} & v_{\mathbf{k}\sigma} \\ v_{\mathbf{k}\sigma} & u_{\mathbf{k}\sigma} \end{pmatrix} \begin{pmatrix} c_{\mathbf{k}\sigma} \\ c_{\mathbf{k}+\mathbf{Q}\sigma} \end{pmatrix}, \quad (11)$$

where $u_{\mathbf{k}\sigma}$ and $v_{\mathbf{k}\sigma}$ are expressed as

$$(u_{\mathbf{k}\sigma}, v_{\mathbf{k}\sigma}) = \left(\frac{i |W_{\mathbf{k}}|}{\sqrt{2E_{\mathbf{k}}(E_{\mathbf{k}} - \varepsilon_{\mathbf{k}\sigma})}}, \sqrt{\frac{E_{\mathbf{k}} - \varepsilon_{\mathbf{k}\sigma}}{2E_{\mathbf{k}}}} \right), \quad (12)$$

with $E_{\mathbf{k}} = \sqrt{\varepsilon_{\mathbf{k}\sigma}^2 + |W_{\mathbf{k}}|^2}$.

Then the 4×4 Hamiltonian in the pure DDW state can be expressed as

$$H = \Psi_{\mathbf{k}}^{\dagger} \begin{pmatrix} E_{\mathbf{k}} & i\lambda_{\mathbf{k}} & 0 & 0 \\ -i\lambda_{\mathbf{k}}^* & -E_{\mathbf{k}} & 0 & 0 \\ 0 & 0 & E_{\mathbf{k}} & i\lambda_{\mathbf{k}}^* \\ 0 & 0 & -i\lambda_{\mathbf{k}} & -E_{\mathbf{k}} \end{pmatrix} \Psi_{\mathbf{k}}, \quad (13)$$

where $\Psi_{\mathbf{k}}^{\dagger} = (\alpha_{\mathbf{k}\uparrow}^{\dagger}, \beta_{\mathbf{k}\downarrow}^{\dagger}, \alpha_{\mathbf{k}\downarrow}^{\dagger}, \beta_{\mathbf{k}\uparrow}^{\dagger})$.

The above Hamiltonian has been block diagonalized to two 2×2 matrices, which are equivalent to the two fully gapped p -wave pairing superconductors with the opposite chiralities. Thus the whole Hamiltonian should be topologically trivial. When the superconducting term is added to the system, the Hamiltonian is written as the 8×8 matrix. According to Ref. [42] one may also define spinless operators, such that an effective four-band p -wave superconductor can be obtained, among which two bands have $i\lambda_{\mathbf{k}}$ pairing, and the other two have $i\lambda_{\mathbf{k}}^*$ pairing. As a result, the whole topological invariant keeps zero in the superconducting state.

From the above analytical results, one may understand that our main results are rather robust and should not depend on the input parameters we considered. While we would like to emphasize that here the d -wave symmetry is anisotropic and will generate two nodal lines. Generally, our main results do not depend on the directions of the DSC order or the DDW order. While if the nodal lines rotate to cross the Weyl points, the system turns to a gapless one and the topological invariant may not be well defined. For this case, our proposal may not work. On the other hand, we need to pinpoint that here a microscopic model should include three parts of the Hamiltonian, i.e., the original DSC superconductor, the Weyl semimetal system, and their tunneling. With a self-consistent calculation the two systems may be coupled through the direct

or the inverse proximity effect [43–46]. Since the cuprate superconductor itself is a gapless system, for the whole system including the cuprate DSC Hamiltonian, the whole band structure should also be gapless. Then it is difficult to analyze the topological feature numerically and analytically. Thus in the present work, the considered model is phenomenologically written through including the DSC pairing term and the DDW term directly into the two-dimensional Weyl semimetal. Neither the possible mixing of the band structures between the cuprate system and the Weyl semimetal, nor the possible inverse proximity effect [44–46] is considered here. This phenomenological approach has been widely used in various proposals of proximately induced topological superconductors [13–17,30–32]. Experimentally, it was indeed reported that the fully gapped topological superconductor may be realized through coupling to a gapless cuprate superconductor [27]. Moreover, it has been proposed that in cuprate superconductors, there may exist two independent interlayer coupling, namely, the single particle hopping effect and the two-particle pair tunneling effect [47–49]. The mixing of the band structure and the inverse proximity effect may be avoided technically by inserting a thin insulating layer between them. Then the single particle hopping and the inverse proximity effect should be negligibly weak. The DSC and the DDW orders are induced to the Weyl semimetal by the two-particle pair tunneling effect [47–49].

It is insightful to investigate the coexistence of the superconducting order with some other possible orders, and compare the numerical results with those for DDW order. We now consider two kinds of spin order, namely ferromagnetic (FM) order and antiferromagnetic (AFM) order, with the corresponding Hamiltonian being expressed as

$$H_{\text{FM}} = \sum_{\mathbf{k}\sigma} \sigma \Delta_{\text{FM}} c_{\mathbf{k}\sigma}^{\dagger} c_{\mathbf{k}\sigma} \quad (14)$$

and

$$H_{\text{AFM}} = \sum_{\mathbf{k}\sigma} \sigma \Delta_{\text{AFM}} (c_{\mathbf{k}\sigma}^{\dagger} c_{\mathbf{k}+\mathbf{Q}\sigma} + \text{H.c.}). \quad (15)$$

In the presence of the FM order, the system in the non-superconducting state is fully gapped and topologically nontrivial. The Hamiltonian is still expressed as a 2×2 matrix in the momentum space. According to Ref. [42], the superconducting Hamiltonian should still be topologically nontrivial. In the presence of the AFM order, the normal state Hamiltonian is expressed as the 4×4 matrix. However, different from the case of the DDW order, here the Hamiltonian cannot be simply block diagonalized and then the topological features should be stable when additional AFM order is added to the system.

Now we study this issue numerically considering when the FM or AFM order coexists with the DSC pairing order. Considering the open boundary condition, the energy bands of the two kinds of coexisting states are plotted in Fig. 6. As is seen, for both cases, there are gapless edge states at $k_y = 0$ and $k_y = \pi$. The numerical results for the energy bands are consistent with the calculations of the topological invariant, namely, we have $\mathcal{N} = 2$ for both coexisting states. Thus the topologically nontrivial behavior is robust and stable when the FM or AFM order is added into the system.

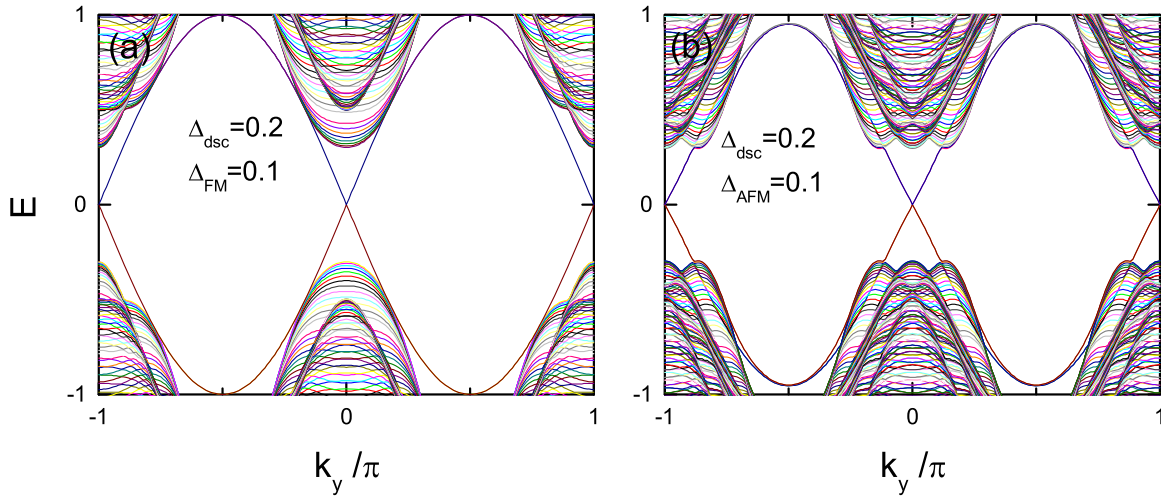


FIG. 6. Energy eigenvalues of the Hamiltonian when the superconducting order coexists with the spin order, with the open boundary condition along x direction being considered.

We here would like to remark on the significance of the present work. First, we have provided a workable method to detect possible weak hidden orders in high- T_c superconductors. Our results may be used to distinguish different pictures of the pseudogap behavior. Second, it has been noted that our minimal model is considered for illustration. One may also choose another topologically nontrivial system to detect other possible competing orders, e.g., if a topological insulator system with time-reversal symmetry is considered, a topological superconductor protected by the time-reversal symmetry may be constructed. This system may be used to detect both the spin order and the DDW order because the time-reversal symmetry is broken by these orders. Moreover, we expect that our scenario may also work well for iron-based superconducting materials. Recently it has been reported the topological superconductor can be realized in the family of iron-based superconductors. And it was widely believed that multiple competing orders may also be important in understanding the superconductivity of this family. At last, we have also provided an effective method to realize the topological superconductor with a high- T_c superconductor platform. The results may be useful in the further studies of topological superconductors and Majorana bound states, which may have potential application in topological quantum computation.

IV. SUMMARY

In summary, we have proposed that the heterostructures may be used to detect the hidden orders in high- T_c superconductors. A typical system, namely a two-dimensional Weyl model in proximity to a high- T_c superconductor with the d -wave pairing order or a possible competing d -density-wave order, is considered to endorse our proposal. For the pure superconducting state, the system is topologically nontrivial and there are gapless edge states crossing the Fermi energy. When an additional d -density wave is added, the system becomes topologically trivial and the edge states are gapped. We elaborate that these features may be detected experimentally through the spectral functions and the local density of states at the system edge. Our results may be helpful for exploring the mechanism of the high- T_c superconductivity.

ACKNOWLEDGMENTS

We thank Wei Chen for helpful discussions. This work was supported by the GRF of Hong Kong (Grants No. HKU173309/16P and No. HKU173057/17P), the Natural Science Foundation from Jiangsu Province of China (Grant No. BK20160094), and the Start-up Foundation from South China Normal University.

-
- [1] J. G. Bednorz and K. A. Müller, *Z. Phys. B* **64**, 189 (1986).
 [2] T. Timusk and B. Statt, *Rep. Prog. Phys.* **62**, 61 (1999).
 [3] E. J. Mueller, *Rep. Prog. Phys.* **80**, 104401 (2017).
 [4] V. J. Emery and S. A. Kivelson, *Nature (London)* **374**, 434 (1995).
 [5] S. Chakravarty, R. B. Laughlin, D. K. Morr, and C. Nayak, *Phys. Rev. B* **63**, 094503 (2001).
 [6] B. Keimer, S. A. Kivelson, M. R. Norman, S. Uchida, and J. Zaanen, *Nature (London)* **518**, 179 (2015).
 [7] E. Fradkin, S. A. Kivelson, and J. M. Tranquada, *Rev. Mod. Phys.* **87**, 457 (2015).
 [8] I. M. Vishik, *Rep. Prog. Phys.* **81**, 062501 (2018).
 [9] J. F. Dodaro, H.-C. Jiang, and S. A. Kivelson, *Phys. Rev. B* **95**, 155116 (2017).
 [10] R.-G. Cai, L. Li, Y.-Q. Wang, and J. Zaanen, *Phys. Rev. Lett.* **119**, 181601 (2017).
 [11] X. L. Qi and S. C. Zhang, *Rev. Mod. Phys.* **83**, 1057 (2011).
 [12] C. Nayak, S. H. Simon, A. Stern, M. Freedman, and S. Das Sarma, *Rev. Mod. Phys.* **80**, 1083 (2008).
 [13] L. Fu and C. L. Kane, *Phys. Rev. Lett.* **100**, 096407 (2008).
 [14] X. L. Qi, T. L. Hughes, and S. C. Zhang, *Phys. Rev. B* **82**, 184516 (2010).
 [15] J. D. Sau, S. Tewari, R. M. Lutchyn, T. D. Stanescu, and S. Das Sarma, *Phys. Rev. B* **82**, 214509 (2010).

- [16] R. M. Lutchyn, J. D. Sau, and S. Das Sarma, *Phys. Rev. Lett.* **105**, 077001 (2010).
- [17] Y. Oreg, G. Refael, and F. von Oppen, *Phys. Rev. Lett.* **105**, 177002 (2010).
- [18] J. R. Williams, A. J. Bestwick, P. Gallagher, S. S. Hong, Y. Cui, A. S. Bleich, J. G. Analytis, I. R. Fisher, and D. Goldhaber-Gordon, *Phys. Rev. Lett.* **109**, 056803 (2012).
- [19] L. P. Rokhinson, X. Liu, and J. K. Furdyna, *Nat. Phys.* **8**, 795 (2012).
- [20] M. T. Deng, C. L. Yu, G. Y. Huang, M. Larsson, P. Caroff, and H. Q. Xu, *Nano Lett.* **12**, 6414 (2012).
- [21] A. Das, Y. Ronen, Y. Most, Y. Oreg, M. Heiblum, and H. Shtrikman, *Nat. Phys.* **8**, 887 (2012).
- [22] V. Mourik, K. Zuo, S. M. Frolov, S. R. Plissard, E. P. A. M. Bakkers, and L. P. Kouwenhoven, *Science* **336**, 1003 (2012).
- [23] J.-P. Xu, M.-X. Wang, Z. L. Liu, J.-F. Ge, X. Yang, C. Liu, Z. A. Xu, D. Guan, C. L. Gao, D. Qian, Y. Liu, Q.-H. Wang, F.-C. Zhang, Q.-K. Xue, and J.-F. Jia, *Phys. Rev. Lett.* **114**, 017001 (2015).
- [24] H.-H. Sun, K.-W. Zhang, L.-H. Hu, C. Li, G.-Y. Wang, H.-Y. Ma, Z.-A. Xu, C.-L. Gao, D.-D. Guan, Y.-Y. Li, C. Liu, D. Qian, Y. Zhou, L. Fu, S.-C. Li, F.-C. Zhang, and J.-F. Jia, *Phys. Rev. Lett.* **116**, 257003 (2016).
- [25] Q. L. He, L. Pan, A. L. Stern, E. C. Burks, X. Che, G. Yin, J. Wang, B. Lian, Q. Zhou, E. S. Choi, K. Murata, X. Kou, Z. Chen, T. Nie, Q. Shao, Y. Fan, S.-C. Zhang, K. Liu, J. Xia, and K. L. Wang, *Science* **357**, 294 (2017).
- [26] P. Zareapour, A. Hayat, S. Yang, F. Zhao, M. Kreshchuk, A. Jain, D. C. Kwok, N. Lee, S.-W. Cheong, Z. Xu, A. Yang, G. D. Gu, S. Jia, R. J. Cava, and K. S. Burch, *Nat. Commun.* **3**, 1056 (2012).
- [27] E. Wang, H. Ding, A. V. Fedorov, W. Yao, Z. Li, Y.-F. Lv, K. Zhao, L.-G. Zhang, Z. Xu, J. Schneeloch, R. Zhong, S.-H. Ji, L. Wang, K. He, X. Ma, G. Gu, H. Yao, Q.-K. Xue, X. Chen, and S. Zhou, *Nat. Phys.* **9**, 621 (2013).
- [28] T. Yilmaz, I. Pletikoscic, A. P. Weber, J. T. Sadowski, G. D. Gu, A. N. Caruso, B. Sinkovic, and T. Valla, *Phys. Rev. Lett.* **113**, 067003 (2014).
- [29] Z. X. Li, C. Chan, and H. Yao, *Phys. Rev. B* **91**, 235143 (2015).
- [30] Z. Yan, F. Song, and Z. Wang, *Phys. Rev. Lett.* **121**, 096803 (2018).
- [31] F. Zhang, C. L. Kane, and E. J. Mele, *Phys. Rev. Lett.* **111**, 056402 (2013).
- [32] Q. Wang, C.-C. Liu, Y.-M. Lu, and F. Zhang, *Phys. Rev. Lett.* **121**, 186801 (2018).
- [33] H. Zhao, B. Rachmilowitz, Z. Ren, R. Han, J. Schneeloch, R. Zhong, G. Gu, Z. Wang, and I. Zeljkovic, *Phys. Rev. B* **97**, 224504 (2018).
- [34] P. Zhang, K. Yaji, T. Hashimoto, Y. Ota, T. Kondo, K. Okazaki, Z. Wang, J. Wen, G. D. Gu, H. Ding, and S. Shin, *Science* **360**, 182 (2018).
- [35] D. Wang, L. Kong, P. Fan, H. Chen, S. Zhu, W. Liu, L. Cao, Y. Sun, S. Du, J. Schneeloch, R. Zhong, G. Gu, L. Fu, H. Ding, and H.-J. Gao, *Science* **362**, 333 (2018).
- [36] C. Liu, X. Qi, X. Dai, Z. Fang, and S. Zhang, *Phys. Rev. Lett.* **101**, 146802 (2008).
- [37] J. Ahn and B.-J. Yang, *Phys. Rev. Lett.* **118**, 156401 (2017).
- [38] S. Nie, H. Weng, and F. B. Prinz, *Phys. Rev. B* **99**, 035125 (2019).
- [39] A. Damascelli, Z. Hussain, and Z.-X. Shen, *Rev. Mod. Phys.* **75**, 473 (2003).
- [40] O. Fischer, M. Kugler, I. Maggio-Aprile, C. Berthod, and C. Renner, *Rev. Mod. Phys.* **79**, 353 (2007).
- [41] T. Zhou, Y. Gao, and Z. D. Wang, *Sci. Rep.* **4**, 5218 (2014).
- [42] T. Zhou and Z. D. Wang, *Phys. Rev. B* **88**, 155114 (2013).
- [43] W. L. Mcmillan, *Phys. Rev.* **175**, 537 (1968).
- [44] V. N. Krivoruchko and E. A. Koshina, *Phys. Rev. B* **66**, 014521 (2002).
- [45] F. S. Bergeret, A. F. Volkov, and K. B. Efetov, *Phys. Rev. B* **69**, 174504 (2004).
- [46] S. Tollis, M. Daumens, and A. Buzdin, *Phys. Rev. B* **71**, 024510 (2005).
- [47] J. M. Wheatley, T. C. Hsu, and P. W. Anderson, *Phys. Rev. B* **37**, 5897 (1988).
- [48] T. Xiang and J. M. Wheatley, *Phys. Rev. Lett.* **76**, 134 (1996).
- [49] T. Zhou, *Phys. Rev. Lett.* **106**, 167001 (2011).